Structure and magnetism of Mn/Ru and Mn/Fe/Mn/Ru superlattices prepared by molecular-beam epitaxy

V. Dupuis,* M. Maurer,† M. Piecuch, M. F. Ravet,‡ J. Dekoster,§ S. Andrieu, and J. F. Bobo
Laboratoire Mixte, Saint Gobain, CRPAM, Boîte Postale 109, 54704 Pont-à-Mousson, France

F. Baudelet‖ and P. Bauer
Laboratoire de Physique des Solides, Université de Nancy 1, Boîte Postale 239, 54506 Vandoeuvre-lès-Nancy, CEDEX, France

A. Fontaine
Laboratoire pour l'Utilisation du Rayonnement Electromagnétique, (LURE), Commissariat à l'Energie Atomique (CEA), MENJS, Bâtiment 209d, 91405 Orsay, France

(Received 11 November 1992; revised manuscript received 31 March 1993)

Our recent study on Fe/Ru superlattices revealed a hexagonal structure, a reduced magnetic moment (1.7 μB) in the plane of the layers, and an antiferromagnetic coupling between the Fe mediated through Ru. We inserted just one plane of manganese between the Fe and the Ru to determine the interface influence on the structural and magnetic properties in Mn/Fe/Mn/Ru superlattices by means of local and selective techniques such as x-ray-absorption and Mössbauer spectroscopy. We describe the growth of Mn on Ru by reflection high-energy electron diffraction and by Auger electron microscopy experiments to realize the superlattices Mn/Ru. Complementary results obtained from x-ray-diffraction and macroscopic magnetization measurements allowed us to quantitatively describe our systems. The Mn structure was found to be identical to the Fe structure in Fe/Ru superlattices. We show that there is no solid solution between Fe and Ru at the interface in Fe/Ru which could be responsible for the four Fe magnetically inactive layers. We obtain the same reduced magnetic moment for the next Fe layer and a moment of few tenths of μB for a Mn layer. Finally we confirm once more the excellent quality of the interface in these superlattices which did not give giant magnetoresistance.

INTRODUCTION

Recent progress in the molecular-beam epitaxy (MBE) of metals offers new ways to fabricate layers and superlattices with metastable structures. We have found that it is possible to grow six pseudomorphic hexagonal atomic iron planes on ruthenium (0001).[1] This Fe phase leads to a volume expansion of more than 11% compared to the other common Fe phases. By realizing monocrystalline Fe/Ru superlattices, we expected to observe perpendicular magnetic anisotropy for low iron thickness and to increase the iron local magnetic moment as a consequence of band narrowing.[2] Surprisingly, not only was the axis of magnetization easy along the iron planes[3] but Mössbauer measurements[4] revealed two-plane-thick magnetically inactive layers. The very high Kondo temperature of Fe in Ru (Ref. 5) and the absence of magnetism in hcp $Fe_{1-x}Ru_x$ solid solutions up to $x=85\%$ could explain this lack of magnetism. X-ray-absorption spectroscopy[6] and anomalous diffusion[7] experiments seemed to show a hexagonal iron stacking sequence.

With a view to trying to answer structural questions and to increase the iron magnetic moment, we substituted ruthenium by fcc iridium, which has the same interatomic distances in the close-packed plane (111) and a non-negligible moment in iron (0.2 μB).[8] Recent magnetic measurements revealed an out-of-plane easy axis.[9] Structural experiments on superlattices of Fe/Ir revealed that fcc iron growth by epitaxy on iridium with similar crystalline parameters as on ruthenium.[10] But conversely to the Fe/Ru case, the Fe/Ir x-ray appearance near-edge structure (XANES) spectra are perfectly isotropic which is surprising considering the in-plane expansion of the Fe-Fe distances compared to the bulk parameters.

The role of ruthenium in the new Fe hp phase seemed to be evident, then we chose to put manganese in place of iron or to insert it at the interface between Fe and Ru in order to probe the interfacial plane structure by means of the x-ray-absorption selectivity. We first studied the growth modes of manganese on a ruthenium buffer deposited on Al_2O_3 sapphire $(11\bar{2}0)$ by means of Auger spectroscopy and reflection high-energy electron-diffraction (RHEED) oscillations, then we studied the structure of monocrystalline superlattices Mn/Ru and Mn/Fe/Mn/Ru by means of x-ray diffraction and absorption and confirming these results by neutron scattering.[11] the good crystallinity without interdiffusion between the species in these superlattices has been proved by inserting just one interfacial ruthenium plane in Mn/Fe/Mn/Ru. The magnetic behavior of these samples was determined by macroscopic magnetization measurements. The outstanding role of Fe in Mn/Fe/Mn/Ru also allowed us to obtain convincing Mössbauer results.

I. EXPERIMENTAL DEVICES

The superlattices were realized below 10^{-10} Torr by MBE in a RIBER EVA 32 chamber described else-

TABLE I. Characteristics of the studied superlattices.

Samples	Number of layers	Buffer	Substrate
1-($Mn_{6.9\ Å}/Ru_{48.5\ Å}$)	9	200 Å Ru	Al_2O_3 ($11\bar{2}0$)
2-($Mn_{4.2\ Å}/Ru_{17.8\ Å}$)	40	217 Å Ru	mica
3-($Mn_{6.3\ Å}/Ru_{14.7\ Å}$)	40	200 Å Ru	Al_2O_3 ($11\bar{2}0$)
4-$Mn_{2\ Å}/Fe_{8\ Å}/Mn_{2\ Å}/Ru_{17\ Å}$	18	200 Å Ru	mica
5-$Mn_{2\ Å}/Fe_{8\ Å}/Mn_{2\ Å}/Ru_{17\ Å}$	70	200 Å Ru	Al_2O_3 ($11\bar{2}0$)

where[12] equipped with two electron guns and quartz microbalances for ruthenium and iron, and a Knudsen cell at 750 °C for manganese. The deposition rate was typically 0.5 Å/s by electron guns and 0.03 Å/s by cell. the sequential growth is achieved at 150 °C to prevent interdiffusion. The different studied superlattices are deposited on a 20-nm-thick (0001) hcp Ru buffer annealed at 500 °C on two different substrates [mica and ($11\bar{2}0$) sapphire]. They are all referenced in Table I. We follow the growth mode of Mn on Ru from the evolution of the LMM Mn and the MNN Ru Auger electron intensities by transferring the sample after each 8-sec time evaporation from the metallization chamber to the analysis chamber for Auger electron spectroscopy (AES) acquisition. The typical Auger electron signal, when measured with a RIBER Mac 2 analyzer, was of 25 μA at 2-keV energy. The evolution of the surface structure of Mn is checked up by RHEED during the growth of the film. We recorded the intensity of the 00 spot intensity by a CCD camera in order to observe possible oscillations occurring in bidimensional growth.[10]

X-ray scattering measurements with the diffraction vector along the superlattice growth axis have been performed on our high-resolution diffractometer in $\theta/2\theta$ mode[13] and showed the periodicity and the crystallinity of the stacking, and the average distances between the superposed planes. X-ray-absorption spectroscopy (XAS) was performed at the LURE in Orsay using the x-ray beam delivered by the DCI storage ring[6] at the Mn K edge (6540 eV) and at the Fe K edge (7112 eV) by electron detection or fluorescence. In this case, the results revealed the distances between first neighbors and their numbers both in and out of the basal plane for each component.

The macroscopic magnetic behavior of the $Mn_{6.3\ Å}/Ru_{14.7\ Å}$ and the $Mn_{2\ Å}/Fe_{8\ Å}/Mn_{2\ Å}/Ru_{17\ Å}$ superlattices (namely 3 and 9) has been determined by a new alternating gradient force magnetometer (AGFM) (Ref. 14) at the Institut d'Electronique Fondamentale at Orsay.

Conversion electron ^{57}Fe Mössbauer spectra have been performed on the $Mn_{2\ Å}/Fe_{8\ Å}/Mn_{2\ Å}/Ru_{17\ Å}$ superlattice using a gas flow (He: 5% CH_4) proportional counter at room temperature. The source drive (^{57}Co in Rh matrix) and data storage were of usual design.[15] The spectra were fitted using standard routines with Lorentzian line shapes.

II. RESULTS

A. Structure

From the evolution of the Auger peak intensities during the deposit of a manganese film on a ruthenium buffer, the characteristic curve (see Fig. 1) was a series of straight lines with breaks at coverage corresponding to the completion of the successive monolayers. The envelope of points corresponding to each complete monolayer is an exponential having the $e^{-x/\lambda}$ form with $\lambda = 7.1$ Å which corresponds to the mean-free path of the sublayer Auger electron through the Mn overlayer. According to simple topological considerations[16] this typical set corresponds to the homogeneous layer-by-layer growth (or Frank–Van der Merwe mode) of Mn on (0001) Ru. These analyses allowed us to rigorously calibrate the manganese cell and we found a deposition rate equal to 2 Å (one monolayer) per 75 sec. This also has been confirmed by RHEED oscillations. In fact the period of an oscillation [see Fig. 2(a)] corresponding to a layer completion is strictly equal to the 75-sec time determined from the AES broken slopes. These two results ensure the assumption of a layer-by-layer growth without interdiffusion between ruthenium and manganese.

From RHEED images, pseudomorphous growth of only two atomic planes of Mn on (0001) Ru buffer at 150 °C was possible. Then a $\sqrt{3}\times\sqrt{3}R\,30°$ surface reconstruction was observed [see Fig. 2(b)], indicating a classical double hexagonal cell. Note that these substructures only fit for a hexagonal cell on the plane. In the case of a

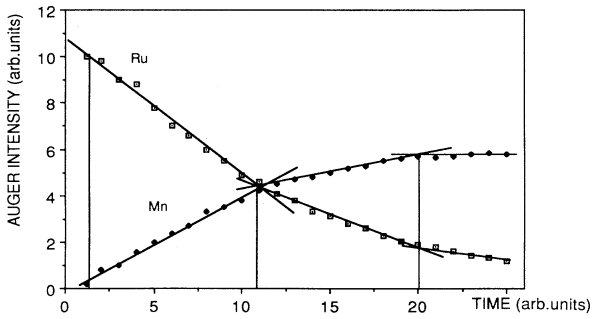

FIG. 1. AES intensities of manganese and ruthenium vs Mn coverage on Ru (0001).

deposit at room temperature, the reconstruction was observed after the seventh atomic plane of Mn. This surface observation does not necessarily reflect the volume tendency after curvature by the following layers. Nevertheless, according to our experimental deposition conditions, we only studied superlattices with thickness Mn film lower or equal to three monolayers.

X-ray-diffraction spectra were exploited at small angles to determine the quality, the period of the modulated structure, and the relative thickness of each component (when there were enough satellites) but also at wide angles to determine the average distance $c/2$ between planes along the growth direction.[17]

For Mn/Ru, the experimental average distance $c/2$ of the superlattice can be described as

$$c=\frac{n_{\mathrm{Mn}}c_{\mathrm{Mn}}+n_{\mathrm{Ru}}+c_{\mathrm{Ru}}}{n_{\mathrm{Mn}}+n_{\mathrm{Ru}}}, \tag{1}$$

where n_{Mn} (resp. n_{Ru}) is the number of Mn planes (respectively, Ru planes) both related by the period value $d=(n_{\mathrm{Mn}}c_{\mathrm{Mn}}+n_{\mathrm{Ru}}c_{\mathrm{Ru}})/2=d_{\mathrm{Mn}}+d_{\mathrm{Ru}}$, we deduced the distance between Mn planes ($c_{\mathrm{Mn}}/2$) by assuming that c_{Ru} is the 4.28-Å classical interreticular distance of the bulk Ru. For the $\mathrm{Mn}_{2\ \text{Å}}/\mathrm{Fe}_{8\ \text{Å}}/\mathrm{Mn}_{2\ \text{Å}}/\mathrm{Ru}_{17\ \text{Å}}$ sample 5 (see Fig. 3) we replaced c_{Mn} in the formula (1) by $\frac{1}{3}c_{\mathrm{Mn}}+\frac{2}{3}c_{\mathrm{Fe}}$, where $c_{\mathrm{Fe}}=4.15$ Å.[1] The $\mathrm{Mn}_{2\ \text{Å}}/\mathrm{Fe}_{8\ \text{Å}}/\mathrm{Mn}_{2\ \text{Å}}/\mathrm{Ru}_{17\ \text{Å}}$ sample 4 deposited on mica was reduced in powder and explored by x-ray diffraction in all its crystallographic directions. No indication for Bragg peaks from an fcc stacking as (200) reflection has been observed. We can conclude to a packing with an ABAB sequence as in the case of Fe/Ru.[1] The estimated d_{Mn} distance is found to be equal to 2.10 Å for all these samples.

We performed XAS measurements on all the samples to evaluate the local distances in the superlattices [from simulation of extended x-ray-absorption fine-structure (EXAFS) oscillations] but also the local symmetry (from XANES fingerprint). Depending on the angle between the electric field of the incident beam and the position vector between the absorber and its first neighbors, the relative weight of the neighbors in plane (respectively, out of plane) is increased for the in-plane polarization (respectively, perpendicular polarization).

Thus the XANES profiles on Mn/Ru and Mn/Fe/Mn/Ru revealed an fcc or hcp-like fingerprint for the polarization in plane in agreement with RHEED observations but a bcc-like behavior for the perpendicular polarization which corresponds to a tetragonal site (see Figs. 4 and 5). This anisotropy leads us to consider a new hexagonal packing more complex than the classical hexagonal compact packing, as in the case of Fe/Ru superlattices previously studied.[6] Note that the perfect isotropy for Fe/Ir superlattices, where the c_{Fe} (equal to 4.20 Å) (Ref. 10) is also strongly dilated, revealed that the c/a ratio (equal to 1.56) far from the ideal hcp ratio (equal to

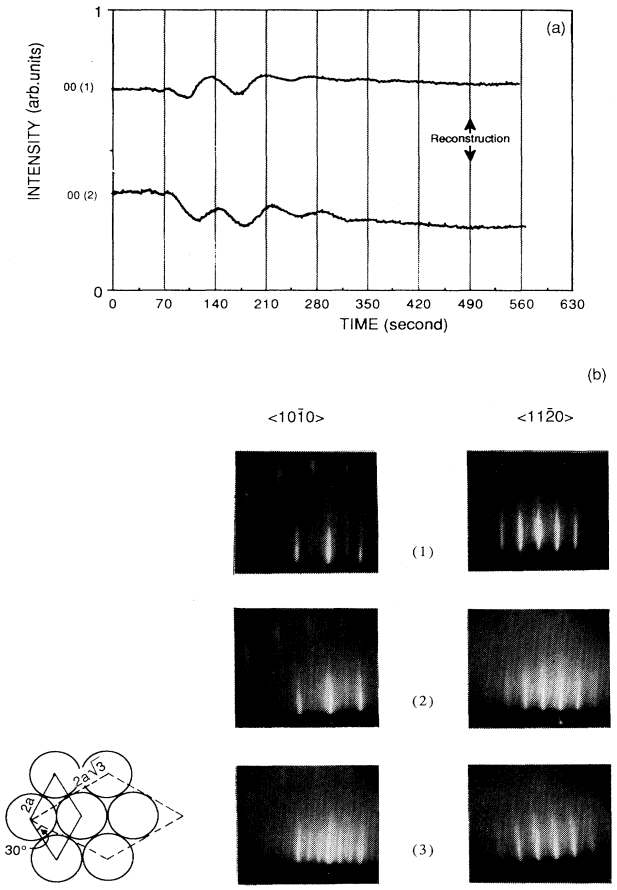

FIG. 2. (a) RHEED oscillations during Mn growth along the (0001) Ru direction at room temperature. (1) and (2) refer to the first and the second most intense central spots, respectively. (b) RHEED patterns at 150 °C substrate temperature of (1) Ru (0001) buffer left ($\langle 10\bar{1}0\rangle$) azimuth and right ($\langle 11\bar{2}0\rangle$) azimuth, (2) after two Mn monolayers, (3) after three Mn monolayers. Notice the extra straight appearance in the $\langle 10\bar{1}0\rangle$ azimuth corresponding to the tripling of the distance between the 0001 and $10\bar{1}0$ nodes in the real space. Finally the little scheme shows the $\sqrt{3}\times\sqrt{3}\ R30°$ surface reconstruction.

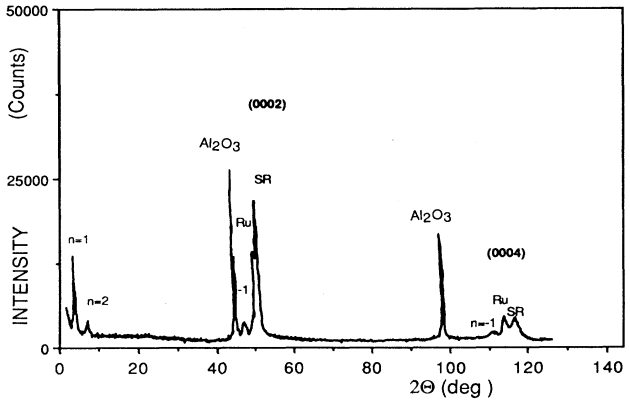

FIG. 3. X-ray scattering $\theta/2\theta$ spectrum on the $(\mathrm{Mn}_{2\ \text{Å}}/\mathrm{Fe}_{8\ \text{Å}}/\mathrm{Mn}_{2\ \text{Å}}/\mathrm{Ru}_{17\ \text{Å}})$ sample 5.

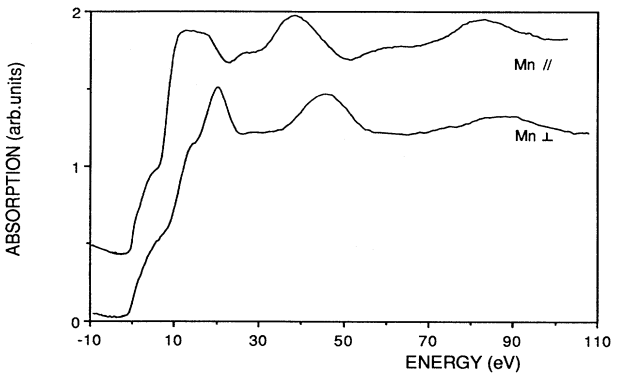

FIG. 4. Anisotropy XANES spectra detected at the Mn edge from in-plane (||) and out-of-plane (⊥) polarization obtained on the $Mn_{4.2\ Å}/Ru_{17.8\ Å}$ sample 2.

1.63) was not due to the XANES anisotropy in Fe/Ru but resulted really from a new hexagonal structure of Fe (or Mn) epitaxially grown on (0001) Ru. In summary, this new packing is supported by the fact that a model with 14 neighbors on two shells for an absorber atom (as in the bcc structure) fit better than a model with only 12 on one shell (as in the hcp or fcc structure), but above all it allowed us to find the same c/a ratio as for x-ray diffraction. It consists of the translation of each dense plane (0001) with respect to the following one, in order to move the gravity center of each triangle to the center of the triangle side [see Fig. 6(a)]. The (0001) new hp plane projection looks like the (110) bcc plane projection with a very small deformation and agrees with the XANES results [see Fig. 6(b)]. The sixfold symmetry observed by RHEED on Fe/Ru appeared as an average between domains with one of the three possible translation directions. Anomalous diffraction shows that the relative intensities of the $(10\bar{1}0)$, $(20\bar{2}0)$, and the $(30\bar{3}0)$ peaks fit well with this new structure.

We now present the EXAFS simulation results on the very interesting sample 5 $Mn_{2\ Å}/Fe_{8\ Å}/Mn_{2\ Å}/Ru_{17\ Å}$. The x-ray-absorption techniques are not only sensitive to the light polarization but also to the local environment of a selective atom species by working at its own absorption edge. Indeed this sample is the ideal one to select the surroundings of just one Mn absorber plane at the interface with Ru neighbors on one hand and with Fe neighbors analogous by their structure on the other one. As for the $Fe_{4\ Å}/Ru_{4\ Å}$ sample previously studied,[6] the first peak of the Fourier transform of the EXAFS spectrum on the $Mn_{2\ Å}/Fe_{8\ Å}/Mn_{2\ Å}/Ru_{17\ Å}$ sample 5 shows a great an-

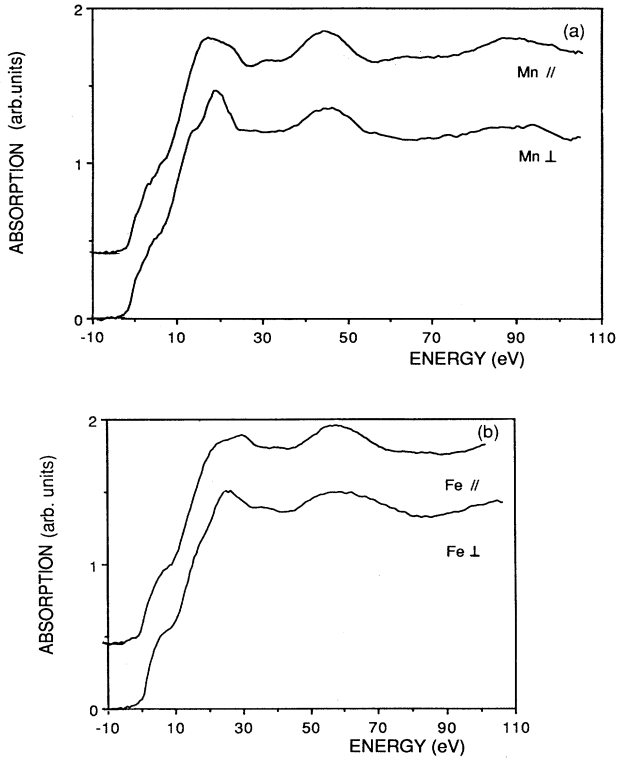

FIG. 5. Anisotropy XANES spectra detected at the Mn (a) and the Fe (b) edge from in-plane (||) and out-of-plane (⊥) polarization obtained on the $Mn_{2\ Å}/Fe_{8\ Å}/Mn_{2\ Å}/Ru_{17\ Å}$ sample 5.

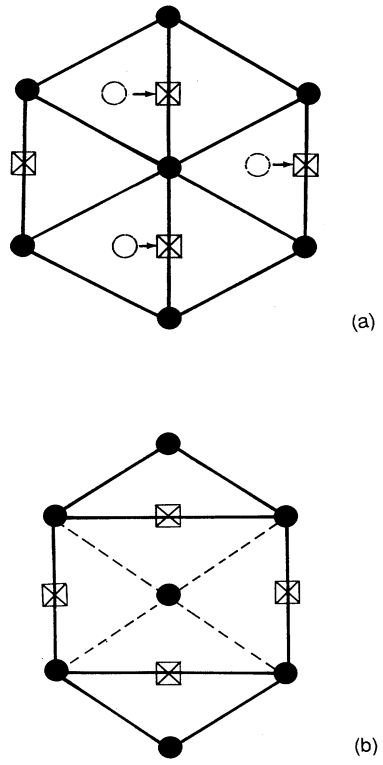

FIG. 6. (a) New hexagonal phase packing $AB'AB'$ obtained by shift of B plane. The number of neighbors is 14 as in the bcc structure. The two out-of-plane distances from a Mn absorber in this new hexagonal packing are $R_1 = 2.50$ Å and $R_2 = 3.15$ Å instead of only one equal to 2.62 Å in the classical hcp. (b) Analogy between the (0001) new hp plane and the (110) bcc plane.

isotropy when the polarization of the x-ray synchrotron emitted beam is in the plane of the superlattice or perpendicular to it [see insert of Figs. 7(a) and 7(b)]. This peak is split when the polarization is close to the c axis which can be explained (as for Fe/Ru samples) (Ref. 6) by considerations of phase shift between Mn and Ru backscatterers for k value around 3 a.u.$^{-1}$. The splitting observed for the parallel polarization comes from the difference between the optical path corresponding at two different Mn-Mn distances.[6] These two splittings in the real space correspond to a beat in the momentum space [see Figs. 7(a) and 7(b)].

With this sample we were able to propose a good qualitative but also quantitative simulation of the EXAFS spectra for both polarizations. The best-fitted values according to those obtained by x-ray-diffraction measurement were obtained by assuming the new hp structure for Mn with respect to those obtained for a classical hcp structure. The deduced c/a is shown in Table II and shows clearly the best agreement between the x-ray-diffraction measurements and the EXAFS new hp model. The c value mentioned in Table II is the average from few experimental EXAFS spectra simulations. The a value for the x-ray diffraction is the tabulated one for the bulk hcp ruthenium.

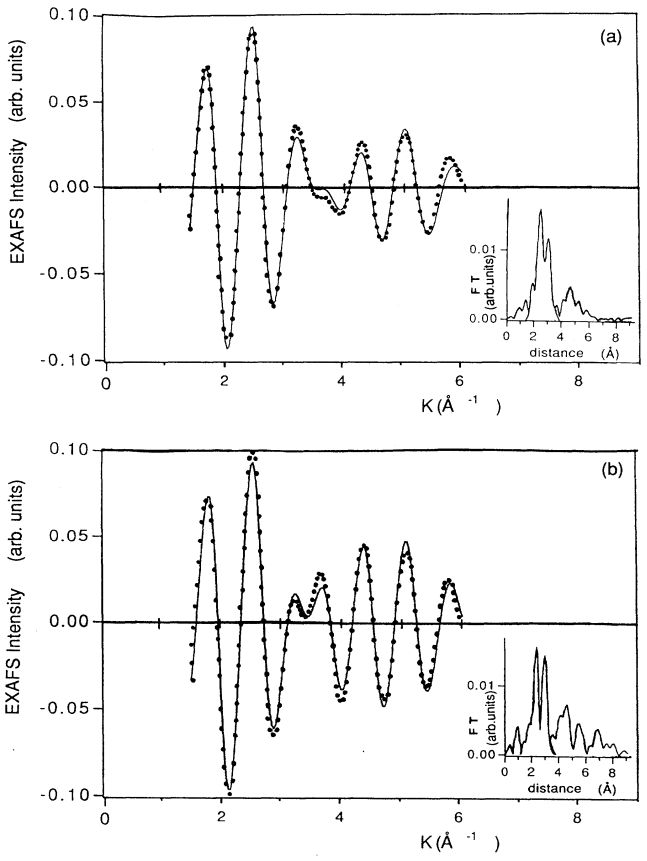

FIG. 7. Experimental (continuous line) and simulated filtered EXAFS oscillations at the Mn edge obtained on the $Mn_{2\ Å}/Fe_{8\ Å}/Mn_{2\ Å}/Ru_{17\ Å}$ sample 5 and detected in two ways. (a) From in-plane polarization, theoretical results are as follows. Fe neighbors out of plane: 0.88 at 2.50 Å and 1.64 at 3.17 Å; 9 Mn neighbors in plane at 2.68 Å; and 1.5 Ru neighbors out of plane at 2.64 Å. Simulated results are as follows. 1.2 Fe neighbors out of plane at 2.51 Å; 9.1 Mn neighbors in plane at 2.71 Å; 1.7 Ru neighbors out of plane at 2.68 Å. (b) From out-of-plane polarization, theoretical results are as follows. Fe neighbors out of plane: 4.2 at 2.50 Å and 2.6 at 3.17 Å; 0 Mn neighbors in plane; 6 Ru neighbors out of plane at 2.64 Å. Simulated results are as follows. Fe neighbors out of plane: 4.35 at 2.56 Å and 2.65 at 3.22 Å; 0 Mn neighbors in plane; 5.9 Ru neighbors out of plane at 2.63 Å. The inserts show the splitting of the Fourier transform.

Notice that for the hcp structure the out-of-plane distance is calculated from the formula $R = a[\frac{1}{4}(c/s)^2 + \frac{1}{3}]^{1/2}$, whereas for the new hp structure we need to consider two out-of-plane distances, namely, $R_1 = [(a/2)^2 + (c/2)^2]^{1/2}$ and $R_2 = [3(a/2)^2 + (c/2)^2]^{1/2}$. The EXAFS spectra simulation evidenced the two characteristic distances R_1 and R_2 instead of only one R and the good weight for each neighbor in agreement with the new hp model (see Fig. 7). For the $Mn_{6\ Å}/Ru_y$ samples 1 and 3, the same structure was accepted according to the fingerprint of XANES spectra but the EXAFS spectra simulations have to integrate the average neighbors of the Mn absorbers. It means that we have two sets of Mn planes: the interfacial Mn planes with Ru and the core Mn planes with only Mn neighbors. The EXAFS oscillations are rapidly attenuated and the simulations are not satisfying. Nevertheless for the $Mn_{4.2\ Å}/Ru_{17.8\ Å}$ sample 2 we found the same value as the $Mn_{2\ Å}/Fe_{8\ Å}/Mn_{2\ Å}/Ru_{17\ Å}$ sample 5 from parallel polarization measurement and R_1 and R_2, respectively, equal to 2.59 Å and 2.87 Å from out-of-plane measurements.

For XAS result comparisons we experimented with a few Mn/Fe superlattices on two different buffers [20-nm-thick (0001): Ru deposited on mica and 75-nm-thick Fe on GaAs (110)]. RHEED structure observations and x-ray-diffraction results were complex and difficult to interpret. Nevertheless the XANES spectra underlined the buffer role. The samples deposited on the Fe buffer show clearly the isotropic classical bcc structure for both iron (essentially from the buffer contribution) and manganese absorber [see Fig. 8(a)]. On the contrary the Ru buffer induced a XANES anisotropy for the Mn layer analogous to that of the previous Mn/Ru or Mn/Fe/Mn/Ru superlattices [see Fig. 8(b)]. The new hp structure of the manganese is transmitted through isotropic (fcc or hcp) Fe layers. These qualitative results represented references for XANES fingerprint depending on the buffer species.

On the other hand, previous neutron-diffraction experiments[11] performed on the ($Mn_{6.3\ Å}/Ru_{14.7\ Å}$) superlattice

TABLE II. Crystallographic parameters obtained for $Mn_{2\ Å}/Fe_{8\ Å}/Mn_{2\ Å}/Ru_{17\ Å}$ sample 5.

Method	a (Å)	$c/2$ (Å)	c/a
x-ray diffraction	2.71	2.10	1.55
EXAFS hcp model	2.71	1.99	1.47
EXAFS hp model	2.71	2.16	1.59

3 confirmed its good periodicity and crystallinity with a doubling of the period due to either an antiferromagnetic coupling of Mn through Ru or noncommensurable period effects.[18] These extra satellites seem to disappear with the magnetic field, but their origin needed to be confirmed by macroscopic magnetization measurements.

B. Magnetism

AGFM magnetization measurements with magnetic field in the plane of the film were performed at room temperature on three characteristic samples: the $Mn_{6.3\ Å}/Ru_{14.7\ Å}$ superlattice 3 (Fig. 9), the $Mn_{2\ Å}/Fe_{8\ Å}/Mn_{2\ Å}/Ru_{17\ Å}$ superlattice 5 [Fig. 10(a)], and a $(Mn_{4\ Å}/Fe_{10\ Å})\times 70$ superlattice deposited on mica with a 20-nm-thick Ru buffer (Fig. 11). They all revealed a magnetic moment increasing with the magnetic film thickness (Fe+Mn) and were characteristic of a weakly antiferromagnetic coupling (coercitive field around 100 Oe). We reported the total moment of the magnetic layer (moment per magnetic atoms times the number of magnetic monolayers) for the three samples on the curve obtained for Fe/Ru samples which have the same hp structure (see Fig. 12). This curve revealed an absence of spontaneous magnetization for Fe layers thinner than four monolayers and a subsequent increase of 1.7 μB per atom in the additional layers.[3] In the case of Mn/Ru and Mn/Fe/Mn/Ru superlattices containing Mn layers we found a reduced moment of a few tenths μB per atom (0.15 μB per atom) for magnetic layers thinner than six monolayers. For the thicker sample $Mn_{4\ Å}/Fe_{10\ Å}$ its value fits well with the previous curve. We can conclude by the presence of some Fe magnetic dead layers as in the case of Fe/Ru samples. Once more we underline the close relationship between the original structure and the magnetic behavior.

^{57}Fe Mössbauer measurements at room temperature have been performed on the Mn/Fe/Mn/Ru sample 5 deposited on sapphire by reflection. The spectrum consists of a quadrupole split doublet with $\Delta Eq = 0.198 \pm 0.003$ mm/s and no sextet magnetic fraction for 8-Å-thick Fe layers [Figure 10(b)]. The isomer shift compared to the α-Fe signal at 300 K is equal to -0.020 ± 0.006 mm/s. The doublet is asymmetric because the c symmetry axis is normal to the surface of the sample and then the Fe atoms are lying in an uniaxial (sixfold) symmetry. Nevertheless the deconvolution of the experimental doublet gives an intensity ratio R equal to 0.56 ± 0.02 mm/s different to the expected one of 0.33 predicted in the case of a perfect texture and an ideal axial symmetry. This re-

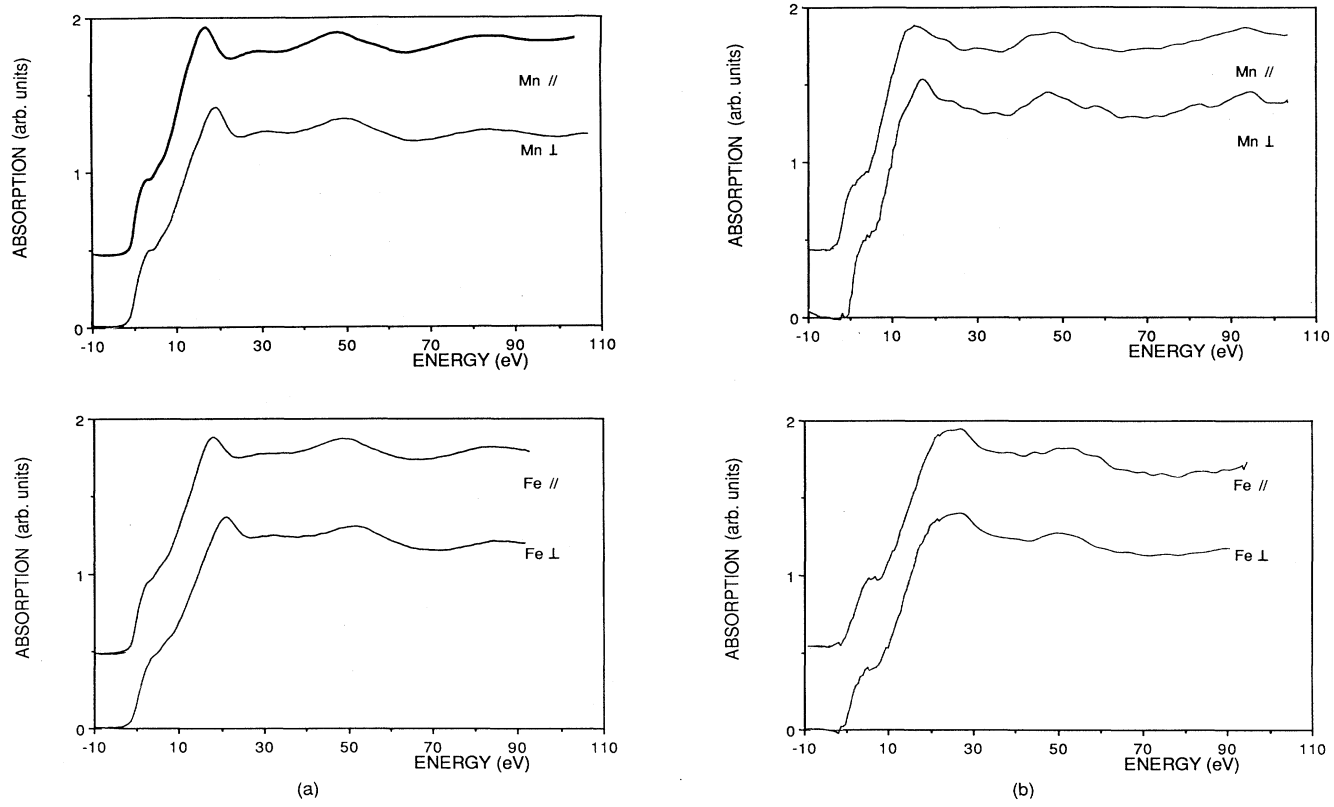

FIG. 8. Buffer influence on XANES fingerprint for Mn/Fe samples at the Mn and the Fe edges. (a) Isotropy of the XANES spectra (|| and ⊥ polarization) obtained on the $Mn_{8\ Å}/Fe_{8\ Å}$ sample deposited on the Fe buffer. (b) Anisotropy of the XANES spectra (|| and ⊥ polarization) obtained on the $(Mn_{4\ Å}/Fe_{8\ Å})$ sample deposited on the Ru buffer.

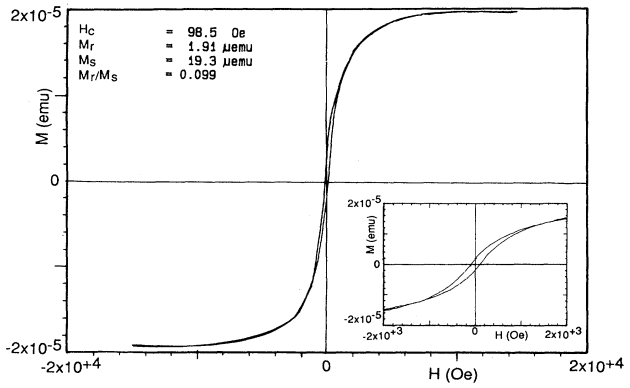

FIG. 9. Hysteresis curve from AGFM obtained at room temperature for the ($Mn_{6.3\ Å}/Ru_{14.7\ Å}$) sample 3 performed with the in-plane magnetic field (insert: zoom of the low-field range).

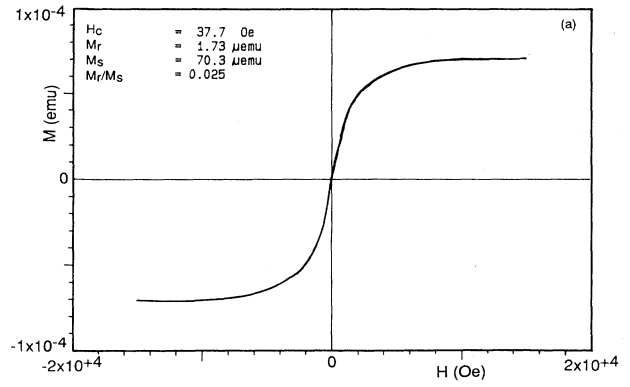

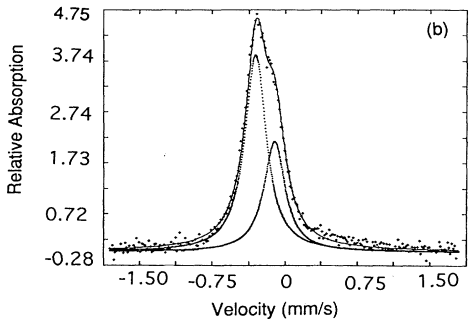

FIG. 10. (a) Hysteresis curve from AGFM obtained at room temperature for the ($Mn_{2\ Å}/Fe_{8\ Å}/Mn_{2\ Å}/Ru_{17\ Å}$) sample 5 performed with the in-plane magnetic field. (b) ^{57}Fe Mössbauer spectrum at room temperature performed with the γ beam normal to the surface of the sample 5.

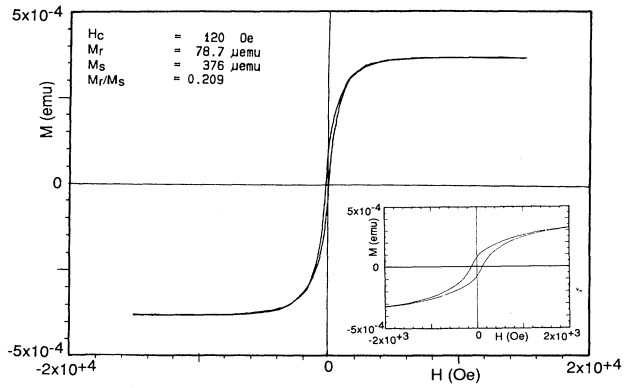

FIG. 11. Hysteresis curve from AGFM obtained at room temperature for the $Mn_{4\ Å}/Fe_{10\ Å}$ sample deposited on the Ru buffer performed with the in-plane magnetic field (insert: zoom of the low-field range).

sult is similar to those obtained on Fe/Ru superlattices where $R = 0.48$ mm/s (Refs. 4,18), and where the sextet magnetic fraction was practically vanishing for Fe thicknesses lower or equal to 8 Å. This analogy allowed us to conclude that an $Fe_{1-x}Ru_x$ solid solution (with $x < 85\%$) at the interface was not responsible for such lack of magnetism. This microscopic result confirmed the previous macroscopic one of weak magnetization for the iron layer. Similar Mössbauer experiments at room temperature on the $Mn_{4\ Å}/Fe_{10\ Å}$ sample on mica by transmission also detected the paramagnetic behavior of the majority of the iron in the 10-Å-thick layer but also its local axial sixfold symmetry (asymmetric quadrupole splitting) and then its hexagonal structure in plane.

In addition, the macroscopic magnetic behavior at low temperature of the $Mn_{4\ Å}/Fe_{10\ Å}$ superlattice deposited on the Ru buffer has been determined by nuclear magnetic resonance (NMR) (Ref. 19) and superconducting quantum interference device (SQUID) magnetometry.[20] The

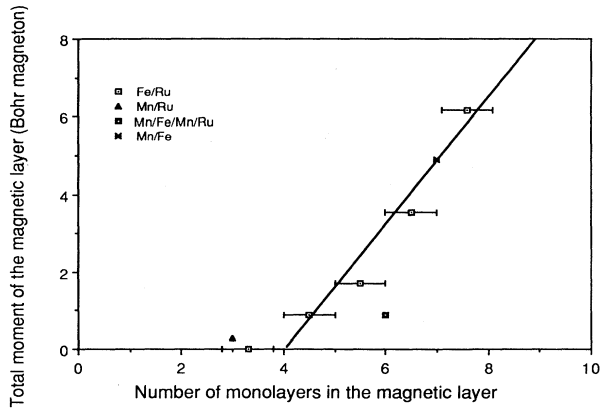

FIG. 12. Total magnetic moment at room temperature vs magnetic thickness for Fe/Ru (⊡); $Mn_{6.3\ Å}/Ru_{14.7\ Å}$ (▲); $Mn_{2\ Å}/Fe_{8\ Å}/Mn_{2\ Å}/Ru_{17\ Å}$ (◙); and $Mn_{4\ Å}/Fe_{10\ Å}$ (✖) samples.

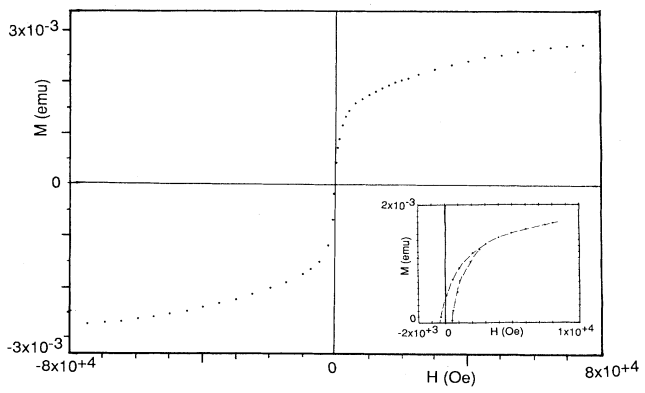

FIG. 13. Hysteresis curve from SQUID magnetometer obtained at 10 K for the ($Mn_{4\ Å}/Fe_{10\ Å}$) sample deposited on the Ru buffer performed with the in-plane magnetic field (insert: zoom of the low-field range).

weak signal of NMR detected in the range of 180–220 MHz at 2 K is used for comparison with the 240 MHz of Mn diluted (0.2%) in bulk iron and showed a very weak diffusion of Mn through Fe. In addition the experimental conditions (rf pulses adjustment to obtain optimum spin echo) underlined an effect of signal amplification characteristic of ferromagnetism, which results from the weak manganese quantity diluted in iron. The magnetic measurements performed at a temperature of 10 K with the magnetic field parallel to the film plane revealed ferromagnetism in layers (large magnetization variation at low field and remanent magnetization Mr/Ms=20%). This gives a saturation magnetization of 1200 emu/cm^3 if we take both Fe and Mn together (which leads to a reduced moment of about 1.6 μB per atom) compared to 1700 emu/cm^3 if we consider that ferromagnetic behavior only comes from Fe layers (2.2 μB per atom as for pure bcc Fe). The cycle (see Fig. 13) showed characteristics of strong antiferromagnetic interactions between layers (magnetization hard to saturate H_s(10 K)=8 T for comparison with H_s(300 K)=1 T and non-negligible coercive field H_c(10 K)=0.5 T. This antiferromagnetic coupling subsists well above the Néel temperature of the spin-density wave state of Mn (100 K) which seems to indicate that this interlayer coupling is related to Mn nonmagnetic layers rather than antiferromagnetic ones but magnetoresistance experiments at low temperature have not revealed giant magnetoresistance as in the case of Fe/Cr.[21] Nevertheless the effect of temperature seems to be very important for such thin layers regarding the decrease of 40% of the magnetization for the Ms(300 K)/Ms(10 K) ratio.

CONCLUSION

The iron substitution in Fe/Ru superlattices previously studied by manganese and its inclusion in Mn/Fe/Mn/Ru allowed us to confirm qualitatively but also quantitatively the new hp stacking evidence by x-ray-absorption measurement. The distance between planes perpendicular to the surface was determined by three complementary techniques (x-ray absorption and diffraction but also neutron scattering). We also showed the persistent structural influence of the buffer on the stacking by studying a few Mn/Fe superlattices.

In addition, some magnetism questions were approached by different techniques such as NMR for Mn, Mössbauer spectroscopy for Fe, and magnetization and neutron scattering under magnetic field. These results revealed an interlayer antiferromagnetic coupling for Mn/Ru and Mn/Fe/Mn/Ru superlattices through thin Ru layers (thinner than 17 Å) and a reduced moment (0.15 μB per atom) for Mn layer (thinner than 7 Å). Concerning the Mn/Fe sample on the Ru buffer we also obtained antiferromagnetic coupling through Mn and we underlined the temperature effect on such superlattices with so thin a period (increase of the magnetic order intralayers and interlayers).

ACKNOWLEDGMENTS

The authors would like to thank P. Veillet from the Institut d'Electronique Fondamentale at Orsay for RMN and SQUID experiments on Mn/Fe samples, and B. George from the Université de Nancy I at Vandoeuvre for magnetoresistance experiments. The Laboratoire Mixte is "Unité Mixte du Centre National de la Recherche Scientifique No. UMR37." The Laboratoire pour l'Utilisation du Rayonnement Electromagnetique is "Unité Associée au Centre National de la Recherche Scientifique."

*Present address: Département de Physique des Matériaux, Université Claude Bernard (Lyon I), Bâtiment 203, 43 Blvd. du 11 Novembre 1918, 69622 Villeurbanne, France.

†Present address: Saint Gobain Les Miroirs, 18 avenue d'Alsace, Cédex 27, 92096 Paris la Défense, France.

‡Present address: Laboratoire de Microstructure et de Microélectronique, Centre National d'Etudes des Telecommunications, 196, avenue H. Ravera, 92220 Bagneux, France.

§Present address: Katholieke Universiteit Leuven, Instituut Voor Kern-en Stralingsfysika, Celestijnenlaan 200 D, B-3001 Leuven, Heverlee, Belgium.

‖Present address: LURE CEA MENJS, Bâtiment 209d, 91405 Orsay, France.

[1]M. Maurer, J. C. Ousset, M. Piecuch, M. F. Ravet, and J. P. Sanchez, Europhys. Lett. **9**, 803 (1989).

[2]P. M. Marcus and V. L. Moruzzi, J. Appl. Phys. **63**, 4045 (1988).

[3]M. Piecuch, M. Maurer, M. F. Ravet, J. C. Ousset, J. M. Broto, and B. Dieny (unpublished).

[4]J. P. Sanchez, M. F. Ravet, M. Piecuch, and M. Maurer, Hyperfine Interactions **57**, 2077 (1990).

[5]D. Riegel, L. Büermann, K. D. Gross, M. Luszik-Bhadra, and S. N. Mishra, Phys. Rev. Lett. **62**, 316 (1989).

[6]F. Baudelet, A. Fontaine, G. Tourillon, D. Gay, M. Maurer, M. Piecuch, M. F. Ravet, and V. Dupuis, Phys. Rev. B **47**, 2344 (1993); F. Baudelet, thesis at LURE, Orsay, France,

1991.

[7]A. De Andres, M. De Santis, D. Raoux, M. Maurer, M. F. Ravet, and M. Piecuch (unpublished).

[8]G. Schütz, R. Wienke, W. Wilhelm, W. Wagner, P. Kienle, R. Zeller, and R. Frahm, Z. Phys. B **75**, 495 (1989).

[9]M. Piecuch, S. Andrieu, J. F. Bobo, M. Maurer, M. F. Ravet, V. Dupuis, J. C. Ousset, and B. Dieny, in *Magnetic Materials: Microstructure and Properties,* edited by T. Suzuki, Y. Sugita, B. M. Clemens, K. Ouchi, and D. Laughlin, MRS Symposia Proceedings No. 232 (Materials Research Society, Anaheim, 1991), p. 165; J. F. Bobo *et al.* (private communication).

[10]S. Andrieu, M. F. Ravet, M. Maurer, V. Dupuis, and M. Piecuch, in *Magnetic Materials: Microstructure and Properties,* edited by T. Suzuki, Y. Sugita, B. M. Clemens, K. Ouchi, and D. Laughlin, MRS Symposia Proceedings No. 232 (Materials Research Society, Anaheim, 1991), p. 159; S. Andrieu, M. F. Ravet, O. Lenoble, V. Dupuis, and M. Piecuch, Europhys. Lett. **18**, 529 (1992).

[11]J. L. Martinez (unpublished).

[12]M. Maurer, J. C. Ousset, M. Piecuch, M. F. Ravet, and J. P. Sanchez, in *Growth, Characterization and Properties of Ultrathin Magnetic Films and Multilayers,* edited by B. T. Jonker, J. P. Heremans, and E. E. Marinero, MRS Symposia Proceedings No. 151 (Materials Research Society, Pittsburgh, 1989), p. 99.

[13]P. Dhez, S. Megtert, M. F. Ravet, and E. Ziegler, Proc. SPIE **984**, 89 (1988).

[14]Apparatus commercialized by the Princeton Measurement Corporation.

[15]C. Janot, *l'Effet Mössbauer et ses Applications à la Physique du Solide et à la Métallurgie Physique* (Editions Masson et Cie, Paris, 1972).

[16]See, for example, B. Carriere and G. Krill, Mat. Sci. Forum **59**, 221 (1990).

[17]M. Piecuch and L. Nevot, Mat. Sci. Forum **59**, 93 (1990).

[18]M. Maurer, M. Piecuch, M. F. Ravet, J. C. Ousset, J. P. Sanchez, C. Aaron, J. Dekoster, D. Raoux, A. De Andres, M. De Santis, A. Fontaine, F. Baudelet, J. L. Rouvière, and B. Dieny, J. Magn. Magn. Mater. **93**, 15 (1991).

[19]K. Le Dang, P. Veillet, C. Chappert, P. Beauvillain, and D. Renard, J. Phys. F **16**, L109 (1986).

[20]Apparatus commercialized by the Metronique Ingenierie.

[21]M. N. Baibich, J. M. Broto, A. Fert, F. Nguyen Van Dan, F. Petroff, P. Etienne, G. Creuset, A. Friederich, and J. Chazelas, Phys. Rev. Lett. **61**, 2472 (1988).

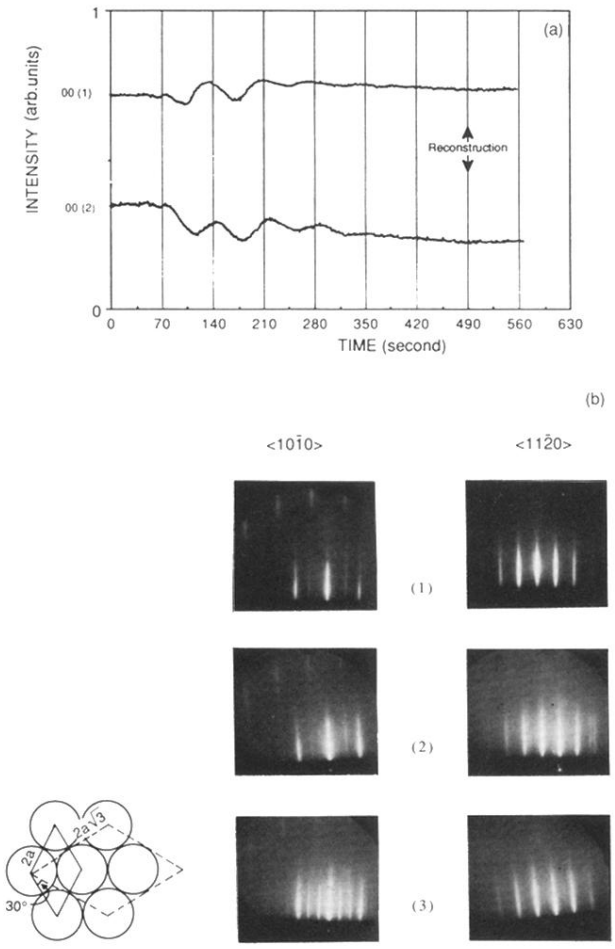

FIG. 2. (a) RHEED oscillations during Mn growth along the (0001) Ru direction at room temperature. (1) and (2) refer to the first and the second most intense central spots, respectively. (b) RHEED patterns at 150 °C substrate temperature of (1) Ru (0001) buffer left ($\langle 10\bar{1}0 \rangle$) azimuth and right ($\langle 11\bar{2}0 \rangle$) azimuth, (2) after two Mn monolayers, (3) after three Mn monolayers. Notice the extra straight appearance in the $\langle 10\bar{1}0 \rangle$ azimuth corresponding to the tripling of the distance between the 0001 and $10\bar{1}0$ nodes in the real space. Finally the little scheme shows the $\sqrt{3} \times \sqrt{3}\, R\,30°$ surface reconstruction.